**Steel and Composite Structures**, *Vol. 28, No. 5 (2018) 559-571*
DOI: https://doi.org/10.12989/scs.2018.28.5.559


# Analysis and design of demountable circular CFST column-base connections

Dongxu Li [*1], Jia Wang [2a], Brian Uy [1b], Farhad Aslani [3c] and Vipul Patel [4d]

[1] *School of Civil Engineering, The University of Sydney, Sydney, NSW 2006, Australia*
[2] *School of Civil and Environmental Engineering, The University of New South Wales, Sydney, NSW 2052, Australia*
[3] *School of Civil, Environmental and Mining Engineering, The University of Western Australia, Crawley, WA 6009, Australia*
[4] *School of Engineering and Mathematical Sciences, La Trobe University, Bendigo, VIC 3552, Australia*

(*Received December 25, 2017, Revised May 7, 2018, Accepted July 3, 2018*)

**Abstract.** In current engineering practice, circular concrete-filled steel tubular (CFST) columns have been used as effective structural components due to their significant structural and economic benefits. To apply these structural components into steel-concrete composite moment resisting frames, increasing number of research into the column-base connections of circular CFST columns have been found. However, most of the previous research focused on the strength, rigidity and seismic resisting performance of the circular CFST column-base connections. The present paper attempts to investigate the demountability of bolted circular CFST column-base connections using the finite element method. The developed finite element models take into account the effects of material and geometric nonlinearities; the accuracy of proposed models is validated through comparison against independent experimental results. The mechanical performance of CFST column-base connections with both permanent and demountable design details are compared with the developed finite element models. Parametric studies are further carried out to examine the effects of design parameters on the behaviour of demountable circular CFST column-base connections. Moreover, the initial stiffness and moment capacity of such demountable connections are compared with the existing codes of practice. The comparison results indicate that an improved prediction method of the initial stiffness for these connections should be developed.

**Keywords:** circular concrete-filled steel tubular column; column-base connection; demountable; finite element analysis; design codes

## 1. Introduction

In recent years, it is well recognized that the construction industry has induced significant negative impacts on the environment. Consequently, the environmental protection and sustainable development have been gaining worldwide awareness. Specific methods for lowering these negative impacts can be achieved through designing demountable structures. Therefore the structural components and materials can be reused rather than recycled (Gorgolewski 2006). Compared with other construction materials, structural steel can be reused many times without compromising material properties and seems to be the most suitable construction material (Winters-Downey 2010). In addition, the reuse of building components is mostly depended on their connections with other components. For the elements connected by using welding or other sealants, the dismantling work requires particular attention, and the time and labour cost would inevitably be increased. On the contrary, bolted connections are encouraged owing to the fact that they can facilitate installing and dismantling of structural buildings in an easy manner and make the structural components reused for their next service life.

Extensive studies on concrete-filled steel tubular (CFST) columns have been carried out due to their significant structural and constructional benefits (Xiao *et al*. 2011 and Uy 2001a). The use of steel tube confines the concrete core and increases the compressive strain capacity and displacement ductility of the concrete (Uy 2001b, Uy *et al*. 2011, Han 2004, Xiong *et al*. 2017). In turn, the infilled concrete restrains the local buckling of the tube. In addition to providing increased flexural stiffness and compressive strength, Uy (2001b) also reported that the construction of CFST columns produced significant savings on material costs when compared with conventional steel columns. Moreover, the lettable floor area can be increased by reducing the required column cross-section size. Therefore, in multi-story buildings, CFST columns are being used as one of the main structural elements to resist both vertical and horizontal loads (Ellobody *et al*. 2006). Although a significant number of studies have been conducted on CFST columns, the work on circular CFST column connections are still very limited, especially for the circular CFST column-base connections.

Hitaka *et al*. (2003) reviewed three most widely used CFST column-base connection designs in Japan. It was found that the embedded CFST column-base connections

*Corresponding author, Research Fellow,
E-mail: dongxu.li@sydney.edu.au
[a] Ph.D. Student, E-mail: jia.wang@unsw.edu.au
[b] Professor, E-mail: brian.uy@sydney.edu.au
[c] Senior Lecturer, E-mail: farhad.aslani@uwa.edu.au
[d] Lecturer, E-mail: v.patel@latrobe.edu.au



ISSN: 1229-9367 (Print), 1598-6233 (Online)

achieved higher rigidity than the bolted base plate connections. Bruneau and Marson (2004) tested four embedded CFST column-base connections under cyclic loading, the ultimate strength and ductility of the connections were determined. The authors concluded that the embedded CFST column-base connections provided an effective mechanism to dissipate seismic energy. Kim *et al*. (2015) proposed a new base plate system using deformed reinforcing bars inside and outside of the column for bolted CFST column-base connections. The cyclic behaviour of the connections was investigated, and it was found that good seismic performance can be achieved providing sufficient anchor bolts were arranged. Hsu and Lin (2006) conducted cyclic tests on five embedded CFST column-base connections with various design details. Seismic performance of the connections was investigated and compared with existing design provisions. More recently, the seismic performance of a series of embedded CFST column-base connections was evaluated by Lehman and Roeder (2012) and Moon *et al*. (2012). Most of the specimens failed with a ductile tearing of steel tubes. The corresponding design criteria were further studied and established by Stephens *et al*. (2016).

In the current construction industry, there is an increasing trend to design structures that can be dismantled. However, most of the existing demountable structures are limited to short-term or small-scale use such as travelling shows, carnival structures and school classrooms. Uy (2014) proposed the concept of demountable structures and indicated demountable structures could be extended to large-scale buildings by utilising bolted connections. In addition, some research into demountable connections for steel-concrete composite structures has already been conducted (Rehman *et al*. 2016, Moynihan and Allwood 2014, Li *et al*. 2017b, 2018). The present paper attempts to develop finite element models to investigate the demountability of bolted circular CFST column-base connections in a typical moment resisting frame, where the typical load on the column will be a combination of axial compression and horizontal displacement. Comparisons between permanent and demountable connections are carried out then. The effects of a few design parameters on the performance of the bolted CFST column-base connections are evaluated using the proposed finite element model. Furthermore, the strength and initial stiffness of the demountable CFST column-base connections are compared with the existing codes of practice.

## 2. Finite element model and verification

### 2.1 Basic concepts

Full-scale experimental studies are the most effective methods for investigating the behaviour of the structural components and reliable results can be obtained. However, the experimental study is costly and time-consuming; it is not feasible to include a wide range of design parameters into the experimental programme. Thereby, the finite element analysis package ABAQUS (2012) was utilised herein to develop an accurate finite element model for predicting the behaviour of bolted CFST column-base connections. The proposed non-linear finite element model can enhance the understanding of the demountable circular CFST column-base connections through analysis of a series of major design parameters. This section utilised existing experimental results that are available from an independent literature review as the database to develop proper finite element model, which will be extended for the prediction of the behaviour of circular CFST column-base connections and further parametric study.

It should be noted that available test results that are suitable for model validation only focused on specimens under a combination of compression and horizontal seismic loading. There is no circular CFST column-base connection test has been tested before under monotonic loading. Thus, considering the consistency of this study, the following finite element model was based on the circular CFST column-base connections under the combination of axial compression and horizontal seismic loading. According to the previous work by Li *et al*. (2016b), it is believed that the major steel components of the connections that can keep elastic and be reused under monotonic loading, once they can be reused under seismic condition.

### 2.2 Element, mesh, interactions, boundary conditions and loading

A typical finite element model of bolted CFST column-base connection is depicted in Fig. 1. As suggested by Mirza and Uy (2010), steel column, infilled concrete, base plate, anchor bolts and concrete foundation were modelled with the three-dimensional solid elements (C3D8R). In this paper, a sensitivity analysis was performed to provide a reasonable mesh size for each modelling part, which can be observed in Fig. 1.

For the bolted CFST column-base connection, the contact interactions are simulated by using "surface-to-surface" contact with a Hard Contact model in the normal direction and a Coulomb Friction model in the tangential direction. As suggested by literature (Eurocode 3 2005 and Li *et al*. 2016a), a friction coefficient between steel-to-concrete and steel-to-steel component was assigned as 0.6 and 0.3, respectively. Moreover, it should be noted the

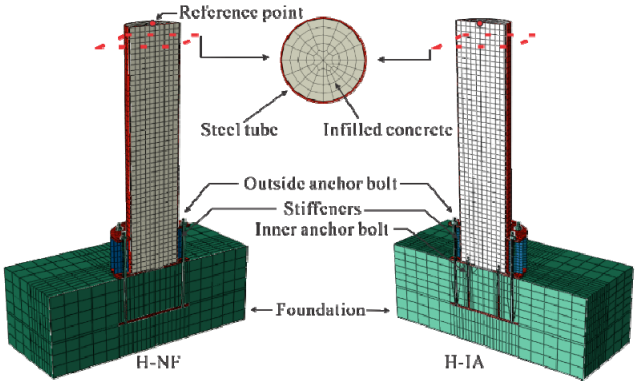


Fig. 1 Finite element model for bolted CFST column-base connections

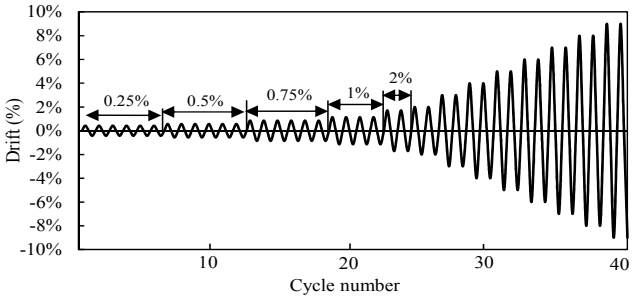


Fig. 2 Cyclic loading sequence

anchor bolt was modelled as a single element, which assumes no friction and slip occurred between the bolt shank and nut, which is based on the observation of the test results. The bottom end of the foundation was constrained with fix-ended boundary condition. All nodes on the top surface of the CFST columns were tied with a centrally located reference point. The axial loads and horizontal deformation were applied to the top reference point. In particular, the ATC-24 (1992) cyclic loading history with 45 cycles was applied in the horizontal direction of the top reference point, as shown in Fig. 2.

### 2.3 Material behaviour

#### 2.3.1 Concrete

A damage plasticity model was used to simulate both confined concrete and unconfined concrete behaviour in compression and tension. Concrete material parameters required being defined include elastic modulus ($E_c$), Poisson's ratio ($v_c$), flow potential eccentricity ($e$), viscosity parameter ($\mu$), dilation angle ($\psi$), shape factor for yield surface ($K_c$), the ratio of initial equibiaxial compressive yield stress to initial uniaxial compressive yield stress ($f_{b0}/f'_c$). These values were determined as suggested by ACI 318 (2010) and Aslani *et al*. (2015). The equivalent stress-strain relationship in compression and tension of the unconfined concrete model proposed by ACI was adopted. For the concrete inside steel tube, a confined concrete model proposed by Tao *et al*. (2013) was utilised. To simulate the concrete behaviour in cyclic loading, damage mechanics material constitutive laws were used. In this analysis, unilateral damage law with two damage variables ($d_t$ and $d_c$) is included to describe the concrete behaviour (Ali *et al*. 2013 and Thai and Uy 2015). In addition, recovery factors $w_t$ and $w_c$ were used to determine the tensile and compressive stiffness recovery. In this analysis, it is assumed that the concrete can regain full stiffness with no damage, and compressive recovery variable ($w_c$) was taken as 1. However, no tensile stiffness was assumed to recover, and tensile recovery variable ($w_t$) was determined to be zero (Li *et al*. 2017a).

#### 2.3.2 Structural steel

The stress-strain relationships of the steel column and base plate are essentially similar. In the present study, a typical tri-linear stress-strain curve was utilised for simulating the behaviour of structural steel. The performance of structural steel under cyclic loading was different from that in monotonic condition due to the Bauschinger effect (Jia and Kuwamura 2014 and Silvestre *et al*. 2015). In this study, a complex three-component nonlinear kinematic rule combined with the isotropic hardening model was used. The determination procedure for various parameters was described by Li *et al*. (2016b).

### 2.4 Verification of finite element model

In this research, two specimens from experimental study tested by Kim *et al*. (2015) were selected to validate the accuracy of the finite element model. Specimens H-NF and H-IA consisted of a circular steel column with diameter and thickness of 518 mm and 9 mm, respectively. The circular base plates utilised by both specimens were identical, with a diameter of 800 mm and thickness of 25 mm. Furthermore, sixteen stiffeners with a height of 375 mm and thickness of 15 mm were used to connect the top and bottom base plates. The only difference between specimens H-NF and H-IA is the application of inner anchor bolts for specimen H-IA, which strongly enhance the energy absorption capability of the connection. The internal anchor bolts can be tightened through a pre-drilled hole on the column wall. The hole is eventually patched with a plate before the infilled concrete casting. The material properties and results comparison of the specimens are shown in Table 1.

#### 2.4.1 Failure modes

To assess the accuracy of the developed numerical model, comparisons of the failure modes between the experimental and finite element analysis results were carried out. Both specimens H-NF and H-IA underwent significant bending deformations, and local buckling of

Table 1 Summary of selected specimens: material properties and results comparison

| Specimen | Specimen details | | | | | | Experimental and finite element results | | |
|---|---|---|---|---|---|---|---|---|---|
| | $f_{y,st}$[1] (MPa) | $f_{y,bp}$[2] (MPa) | $f_{y,iab}$[3] (MPa) | $f_{y,oab}$[3] (MPa) | $f'_{c,col}$[4] (MPa) | $f'_{c,f}$[4] (MPa) | $F_{exp}$ (kN) | $F_{FEM}$ (kN) | $F_{exp}/F_{FEM}$ |
| H-NF | 320 | 320 | - | 562 | 27 | 40 | 405 | 409 | 0.99 |
| H-IA | 320 | 320 | 540 | 562 | 27 | 40 | 455 | 424 | 1.07 |

[1] $f_{y,st}$ is the yield strength of steel tube
[2] $f_{y,bp}$ is the yield strength of base plate
[3] $f_{y,iab}$ and $f_{y,oab}$ is the yield strength of inner and outer anchor bolts, respectively
[4] $f_{c,col}$ and $f'_{c,f}$ is the compressive strength of infilled column concrete and foundation concrete, respectively

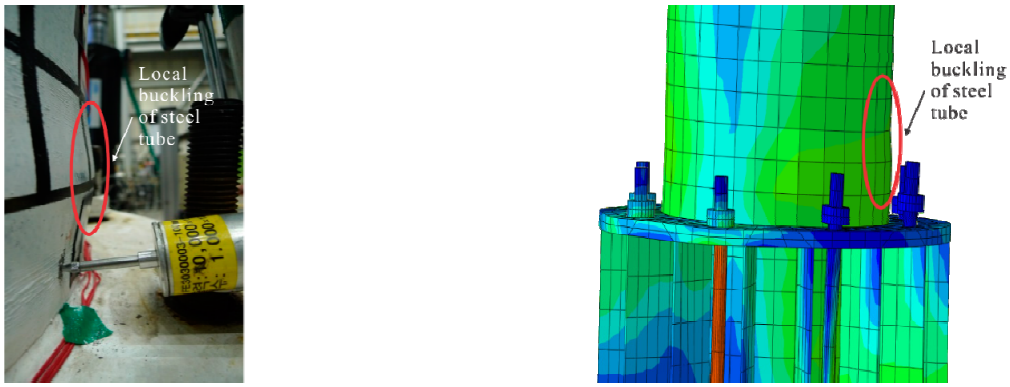


(a) Specimen H-NF

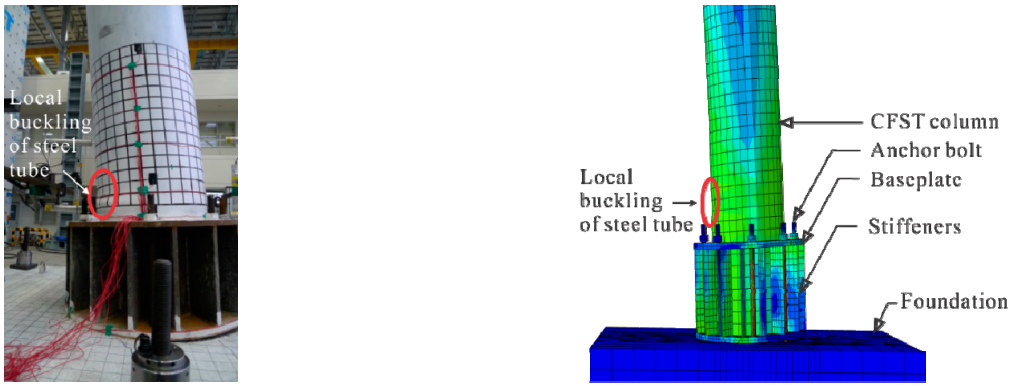


(b) Specimen H-IA

Fig. 3 Final state and failure modes of the specimens

steel tubes occurred near the base plates. Fig. 3 presents the final state and failure modes of the selected specimens. The proposed finite element model provides a reasonable prediction of the local buckling of the steel tubes. Moreover, the outside anchor bolts experienced significant deformations on the compression side.

#### *2.4.2 Hysteretic curves and skeleton curves*

In addition to the final state failure modes, comparisons of hysteretic and skeleton curves between experiment and finite element analysis further demonstrated the accuracy of the developed numerical model. The lateral displacement and reaction force response at the top tip of the CFST column was recorded by Abaqus. The load-displacement relationships of the connections under seismic and monotonic loading were plotted with the recorded results. Specimen H-NF installed outside anchor bolts around the CFST column only, and the poor seismic performance and energy absorption capacity of this connection was observed. On the contrary, specimen H-IA arranged both inner and outside anchor bolts for the CFST column-base connection. Therefore, part of the uplift effect was distributed to the inner anchor bolts, and the ultimate strength capacity was increased by 12%. Moreover, the rigidity and energy dissipation capacity of the connection was significantly enhanced, which can be observed in Fig. 4.

Moreover, for the ease of observation and comparison, skeleton curves obtained from combining peak points of each cycle of load-displacement curves were presented in Fig. 4. It can be seen that the stiffness degradation obtained from the finite element model agreed well with that from the experimental study. The ultimate strength and post-peak behaviour of the connections were simulated accurately, which can be demonstrated by the values of $F_{exp}/F_{FEM}$ in Table 1.

## 3. Comparison of design details

### *3.1 General*

Typical bolted circular CFST column-base connection consists of a base plate welded to the bottom end of the steel tube by full penetration butt welds. Afterwards, the steel tube and base plate are attached to the foundation through a number of anchor bolts. For ease of construction, simple square base plates are commonly used for CFST columns. Axial load and applied moment are transmitted from the CFST columns to the substructures through these connections. Connections with both design details shown in Fig. 5 have found their application in the current construction practice. However, with the design details shown in Fig. 5(a), where the infilled column concrete is continuous to the foundation, dismantling of the connections is infeasible, and the structural components are difficult to be reused. Therefore, the demountable design details shown in Fig. 5(b) are encouraged. In this study, the validated finite element model was utilised to compare the mechanical performance of bolted CFST column-base connections with design details shown in Fig. 5.

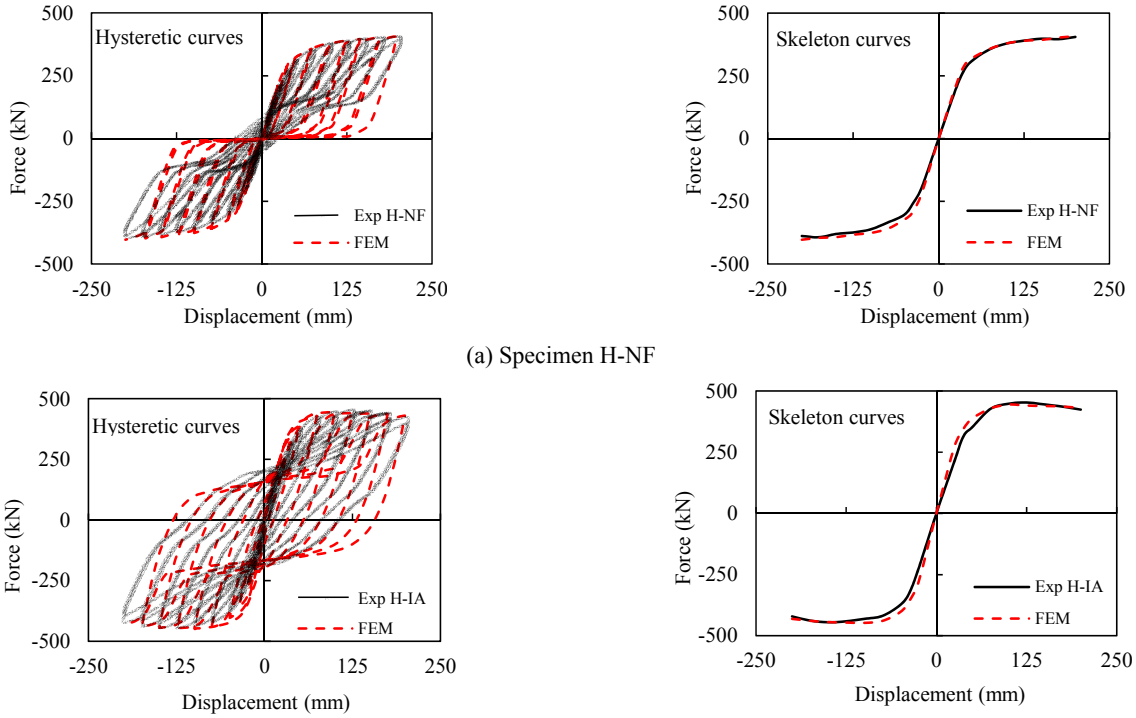


(a) Specimen H-NF

(b) Specimen H-IA

Fig. 4 Hysteretic curves and skeleton curves comparison

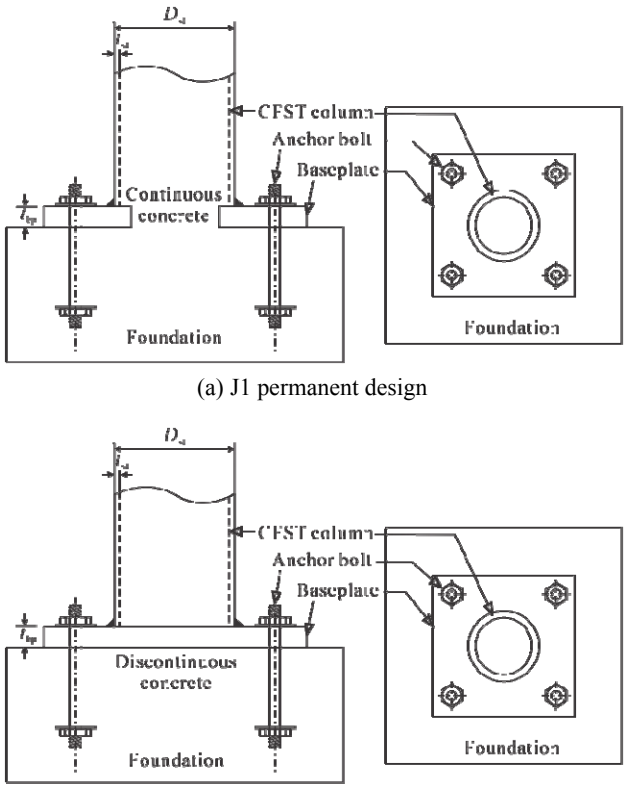


(a) J1 permanent design

(b) J2 demountable design

Fig. 5 Current engineering practice for bolted CFST column-base connections

Specifically, the steel tube used has an outer diameter and tube thickness of 518 mm and 9 mm, respectively. The dimension of the base plate is 800 mm in width and depth and 25 mm in thickness. Four M30 high- strength anchor bolts with the yield strength of 560 MPa were arranged at the corners of the base plate to transmit axial compression, bending moment and shear force to the foundation.

### *3.2 Comparison of strength, ductility and initial stiffness*

Load-displacement curves of both connections were obtained from the numerical model, which are further compared in Fig. 6. It can be observed from the figure that the initial stiffness of both connections was similar, the load-displacement curve for connection J2 indicates higher secant stiffness and 15% higher strength capacity. Moreover, it can be found that the anchor bolts yielded before the yielding of steel tubes and base plates. This phenomenon is mainly due to the use of thick base plates, which significantly delayed the yielding and large plastic deformation of base plates. However, the anchor bolts still sustained tensions until fracture occurred. They were not accounted for reuse and recycling since the steel amount took up a small portion of the whole steel structure. Therefore, the demountable force at which the major steel components start to yield is defined as $F_{dem}$, as shown in Fig. 6(a). In this study, major steel components include steel tube and welded base plate only. Therefore, the first yield of either steel tube or base plate is regarded as the demountable force. Similarly, the demountable moment $M_{dem}$ corresponds to the demountable force by multiplying with the column height.

The initial stiffness of the column-base connection generally has greater influences than other connections on

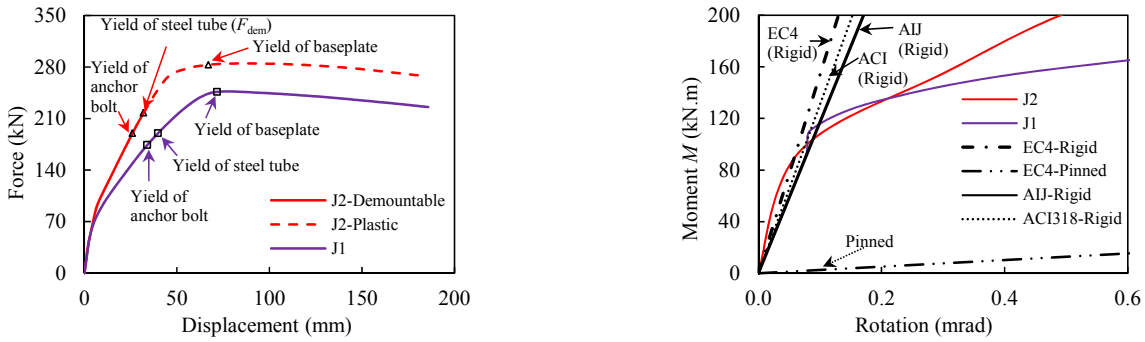


(a) Mechanical performance (b) Initial stiffness

Fig. 6 Comparison of the connections J1 and J2

the performance of the moment resisting frame. It is therefore important to evaluate the rigidities of both connections shown in Fig. 5, and classification of the behaviour of these connections was performed in this study. For the frame construction where the story's sway is not prevented, the column-base connection might be classified according to the Eurocode 3 (2005) and Eurocode 4 (2004). In the present study, the CFST column-base was assumed to be part of the non-bracing frame, and the corresponding rigidity limit can be calculated with Eq. (1).

$$s_{j,ini} = 30E_cI_c / L_c \quad (1)$$

where $L_c$ is the height of the column, $E_c$ and $I_c$ is the elastic modulus and second moment of area of the column, respectively. As suggested by Eurocode 4 (2004), $E_cI_c = E_sI_s + 0.6E_{con}I_{con}$, with $E_s$ and $E_{con}$ representing the elastic modulus of the steel tube and infilled concrete, respectively. Similarly, $I_s$ and $I_{con}$ are the second moment of area for steel tube and infilled concrete, respectively. Research conducted by Aslani *et al*. (2016) indicated that AIJ (1997) and ACI 318 (2008) could better predict the flexural behaviour of composite columns with the following equation $E_cI_c = E_sI_s + 0.2E_{con}I_{con}$. Due to the different definitions of the elastic modulus of the steel and concrete, small discrepancy between AIJ (1997) and ACI 318 (2008) exists. The initial stiffness of connections J1 and J2 was compared with various design provisions. It can be found from Fig. 6(b) that the initial stiffness of connection J1 is about 20% lower than that of connection J2. Moreover, the stiffness of connection J2 is slightly higher than the rigid limit defined by AIJ (1997) and ACI 318 (2008).

### 3.3 Demountability

Li *et al*. (2016a) indicated that the elasticity of a steel component was characterised by its ability to sustain elastic deformation without undergoing the large plastic deformation. The demountability of a typical bolted circular CFST column-base connection depends on the elasticity of the steel column and base plate. The demountability of such connections cannot be achieved with the large plastic deformation occurred in the column or base plate. Fig. 7 depicts the final state of the steel column and base plate for

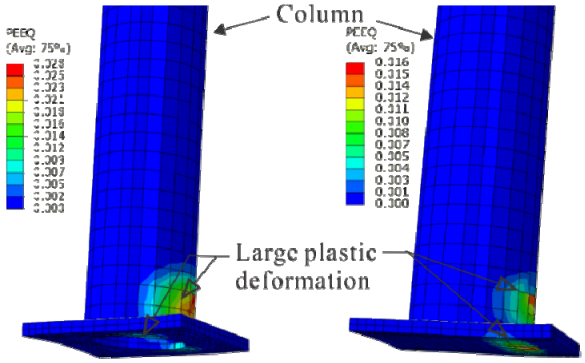


(a) Equivalent plastic deformation of J1 (b) Equivalent plastic deformation of J2

Fig. 7 Final state of steel column and base plate for connections J1 and J2

the bolted CFST column-base connections with different design details. As can be seen, large plastic deformation occurred in the column and base plate of the connections. PEEQ in the figure represents an equivalent plastic strain, which can be regarded as the accumulated plastic strain of the steel members. In this study, steel columns and base plates cannot be reusable if PEEQs of the steel members are greater than zero. According to this criterion, the behaviour of connection J2 with respect to its load-displacement curve can be classified as demountable and plastic segments, as presented in Fig. 6(a). As mentioned above, yielding of anchor bolts will not be accounted for the demountability of circular CFST column-base connections. Thus, the demountable point of the load-displacement curve is determined according to the initiation of the steel tube or base plate yielding. In addition, it should be noted that the connection J1 could not be dismantled and reused, due to the continuous of concrete at the connection region.

By comparing the mechanical performance of the connections J1 and J2, it can be found that the connection J2 exhibited higher ultimate strength and secant stiffness than those of connection J1. In addition to the better mechanical performance, the demountability of the connection and reusability of structural steel also encouraged the connection J2 to be widely applied in the engineering practice.

Table 2 Parametric studies for finite element analysis

| Specimen | $f_{y,bp}$ | $f_{y,ab}$ | $\beta$[1] | $D_{bp}/D_{st}$[2] | $t_{st}/t_{bp}$[3] | $n$[4] | $M_u$[5] | $M_{dem}$[6] | $M_{dem}/M_u$ |
|---|---|---|---|---|---|---|---|---|---|
| | (MPa) | (MPa) | - | - | - | - | (kN) | (kN) | - |
| PS-1 | 250 | 520 | 0.1 | 1.5 | 5.5 | 2 | 695 | 540 | 0.78 |
| PS-2 | 350 | 520 | 0.1 | 1.5 | 5.5 | 2 | 720 | 540 | 0.75 |
| PS-3 | 450 | 520 | 0.1 | 1.5 | 5.5 | 2 | 735 | 540 | 0.73 |
| PS-4 | 320 | 225 | 0.1 | 1.5 | 5.5 | 2 | 475 | 450 | 0.95 |
| PS-5 | 320 | 600 | 0.1 | 1.5 | 5.5 | 2 | 735 | 560 | 0.76 |
| PS-6 | 320 | 830 | 0.1 | 1.5 | 5.5 | 2 | 887 | 562 | 0.63 |
| PS-7 | 320 | 320 | 0.0 | 1.5 | 5.5 | 2 | 562 | 560 | 1.00 |
| PS-8 | 320 | 320 | 0.1 | 1.5 | 5.5 | 2 | 712 | 545 | 0.77 |
| PS-9 | 320 | 320 | 0.2 | 1.5 | 5.5 | 2 | 824 | 524 | 0.64 |
| PS-10 | 320 | 320 | 0.4 | 1.5 | 5.5 | 2 | 813 | 475 | 0.58 |
| PS-11 | 320 | 320 | 0.1 | 1.5 | 5.5 | 2 | 712 | 545 | 0.77 |
| PS-12 | 320 | 320 | 0.1 | 1.5 | 5.5 | 3 | 906 | 591 | 0.65 |
| PS-13 | 320 | 320 | 0.1 | 1.5 | 5.5 | 4 | 925 | 597 | 0.65 |
| PS-14 | 320 | 320 | 0.1 | 1.3 | 5.5 | 2 | 681 | 531 | 0.78 |
| PS-15 | 320 | 320 | 0.1 | 1.5 | 5.5 | 2 | 712 | 545 | 0.77 |
| PS-16 | 320 | 320 | 0.1 | 1.7 | 5.5 | 2 | 734 | 551 | 0.75 |
| PS-17 | 320 | 320 | 0.1 | 1.9 | 5.5 | 2 | 758 | 562 | 0.74 |
| PS-18 | 320 | 320 | 0.1 | 1.5 | 3.3 | 2 | 530 | 410 | 0.77 |
| PS-19 | 320 | 320 | 0.1 | 1.5 | 4.4 | 2 | 659 | 499 | 0.76 |
| PS-20 | 320 | 320 | 0.1 | 1.5 | 5.5 | 2 | 712 | 545 | 0.77 |
| PS-21 | 320 | 320 | 0.1 | 1.5 | 6.6 | 2 | 776 | 586 | 0.76 |

[1] $\beta$ is the level of axial load applied on top of the CFST column
[2] $D_{bp}/D_{st}$ is the ratio of base plate depth to steel tube depth
[3] $t_{st}/t_{bp}$ is the ratio of steel tube thickness to base plate thickness
[4] $n$ is the number of anchor bolts on tension side
[5] $M_u$ is the ultimate moment capacity of the column-base connection obtained from finite element results
[6] $M_{dem}$ is the moment where yielding of major steel components commenced

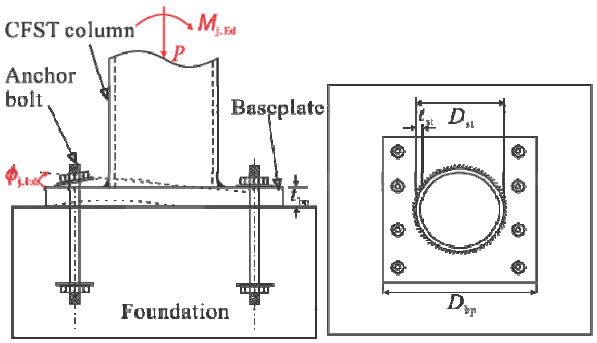


Fig. 8 Illustration of geometric details varied in parametric studies based on connection J2

## 4. Parametric study

This paper attempts to enhance the understanding of the behaviour of demountable circular CFST column-base connections through extensive parametric studies. The authors herein take into account six different variables, and a series of analyses were conducted with one parameter varied each time, according to Fig. 8 and Table 2. It is worth noting that the design parameters relevant to the CFST columns were also investigated, such as column concrete strength, steel tube yield strength and depth-to-thickness ratio of steel tube. However, due to the limited effects on the moment-rotation curves, the results of these parametric studies are not presented. Moreover, demountable moment capacity ($M_{dem}$) is mentioned in the following sections, which means at that particular moment, steel tube and base plate are within elastic range and thus demountable.

### *4.1 Effects of base plate yield strength*

In this analysis, the base plates with different yield strengths were used to investigate the influences on the moment-rotation curves of the bolted circular CFST column-base connections. In addition, the various base plate yield strength was limited to the mild steel, which had a similar mechanical performance and can be accurately simulated with the developed model. As shown in Fig. 9(a), the increase in base plate yield strength significantly improved the ductility of the connections after the peak load

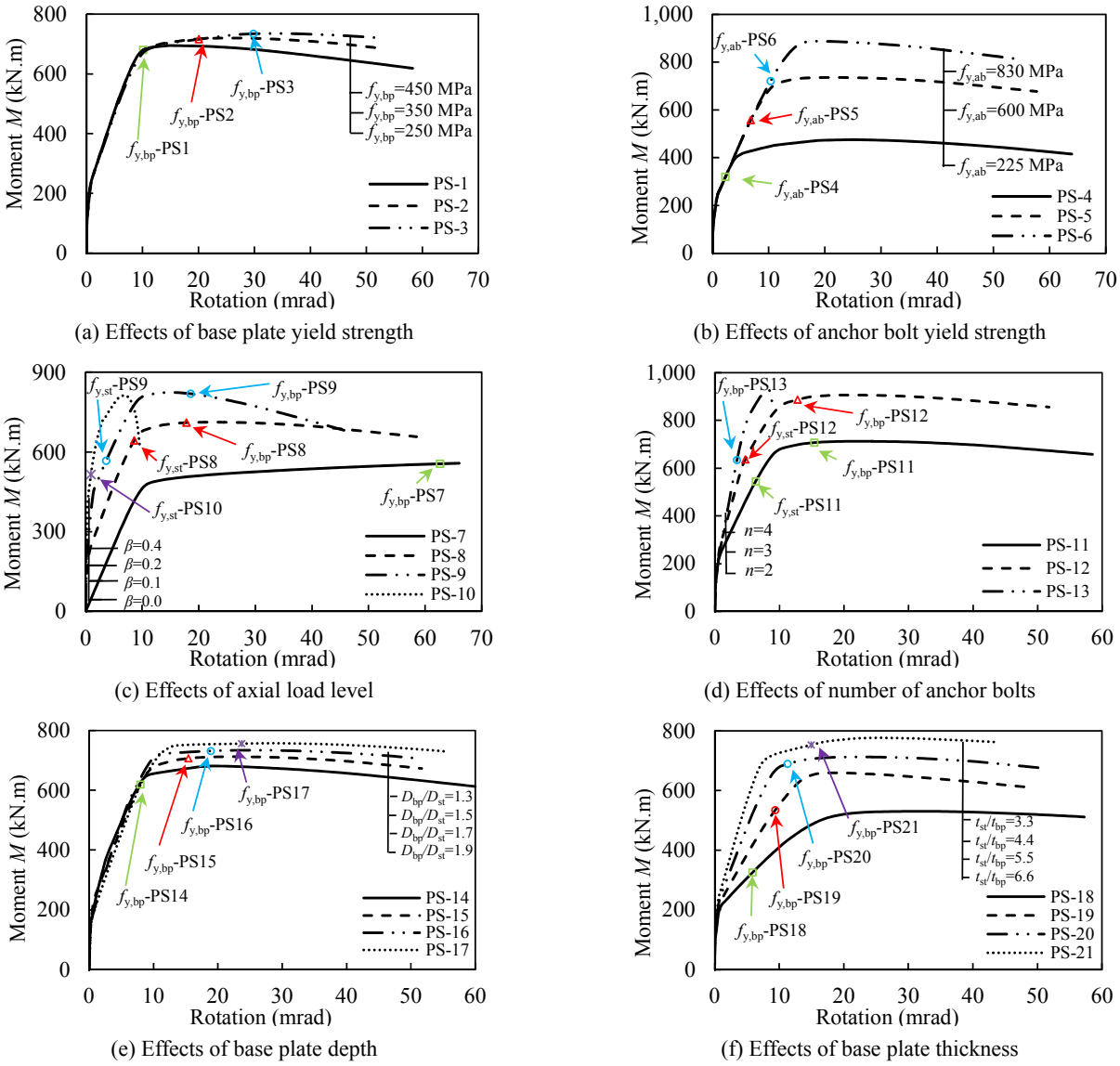


(a) Effects of base plate yield strength

(b) Effects of anchor bolt yield strength

(c) Effects of axial load level

(d) Effects of number of anchor bolts

(e) Effects of base plate depth

(f) Effects of base plate thickness

Fig. 9 Results of parametric studies

was achieved.

Moreover, the ultimate moment capacity was increased by 6% when increasing base plate yield strength from 250 to 450 MPa. For connections SP-1 to SP-3, the anchor bolts in the tension side reached yielding prior to the yielding of steel tubes. Furthermore, the moment capacities of these connections were the same when the yielding of steel tubes commenced, where a demountable moment capacity ($M_{dem}$) was defined accordingly.

### *4.2 Effects of anchor bolt yield strength*

In the current Australian market, three different kinds of anchor bolt are available, namely Class 4.4, Class 8.8 and Class 10.9. The characteristic yield strength of these anchor bolts is 225 MPa, 600 MPa and 830 MPa, respectively. To analyse the effects of anchor bolt yield strength on the performance of the bolted circular CFST column-base connections, anchor bolts with the material properties shown in Table 2 are used. It can be seen from Fig. 9(b) that increasing anchor bolt yield strength had limited influences on the initial stiffness and post-peak behaviour. On the contrary, the ultimate moment capacity was significantly improved by 85% when replacing Class 4.4 bolts with Class 10.9 bolts. The demountable moment capacity of these connections depended on the yielding of steel tubes, which commenced before base plates. As shown in Table 2, this demountable moment capacity ($M_{dem}$) can be increased by using high-strength anchor bolts to some extent. However, when further increasing anchor bolt yield strength from 600 MPa to 830 MPa, the demountable moment capacity of the connection was not significantly increased due to the occurrence of steel tube yielding.

### *4.3 Effects of axial load level*

Four different axial load level were used in this analysis which included $P/P_u$ = 0.0, 0.1, 0.2 and 0.4. It is shown in Fig. 9(c) that increasing axial load level can increase initial stiffness and ultimate moment capacities of the connections.

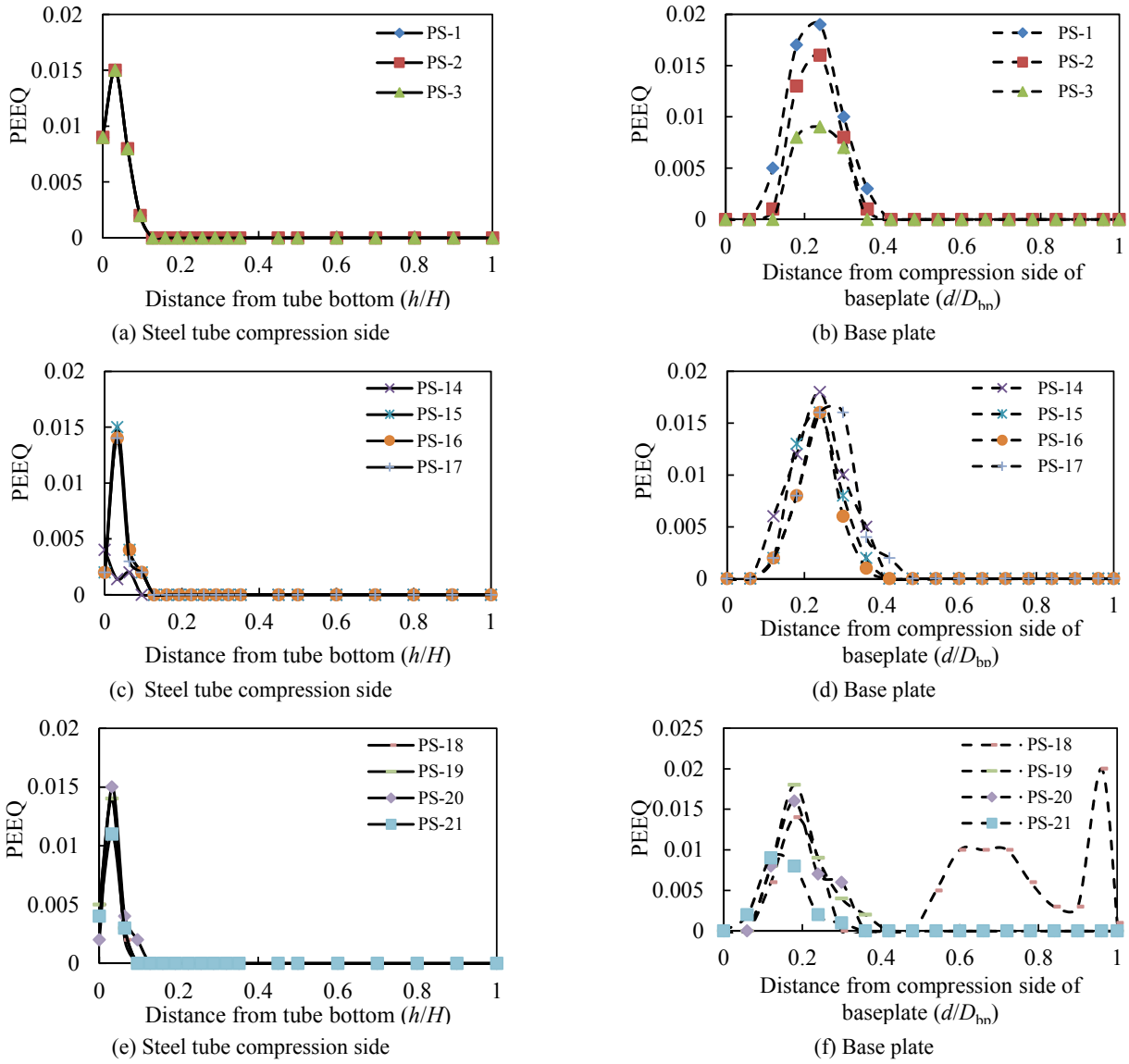


(a) Steel tube compression side (b) Base plate

(c) Steel tube compression side (d) Base plate

(e) Steel tube compression side (f) Base plate

Fig. 10 PEEQ distribution on steel tubes and base plates for selected connections

However, this trend is limited to a certain extent, where axial load level reached 0.4, and significant local buckling of steel tube was observed, which will decrease the ultimate moment capacity and post-peak behaviour of the connection. As shown in Fig. 9(c), only the yield of base plate can be observed when the axial load level is zero. In addition, the yielding of steel tubes prior to that of base plates can be observed for the cases where axial load level ranged from 0.1 to 0.2.

Further increase the axial load level to $\beta = 0.4$, the steel tube underwent large plastic deformation due to the local buckling near the bottom. Under this loading scenario, steel tube underwent plastic deformation at an early stage, while the base plate was still within its elastic range to the end of analysis.

### *4.4 Effects of number of anchor bolts*

Connections SP-11 to SP-13 were used to evaluate the influence of the number of anchor bolts on the mechanical performance and the demountable moment of bolted circular CFST column-base connections. As illustrated in Fig. 9(d), arranging three anchor bolts at the tension side of the connection lead to a 30% increase in ultimate moment capacity, compared to SP-11 where only two anchor bolts were placed on the tension side. Nevertheless, the behaviour of connection SP-13 was not affected significantly, when arranging four anchor bolts on tension side. This phenomenon is mainly attributed to the fact that the anchor bolts resisted high-level bending moment, which is greater than the capacity of the base plate. Therefore, the yielding and large plastic deformation of base plate were to be expected before the yielding of CFST columns.

### *4.5 Effects of base plate depth*

Base plates with various dimensions have been applied in the developed finite element model to study its influences on the moment-rotation curves of the column-base connections. To quantify the design parameter for future design guidance, the base plate depth was normalised as the

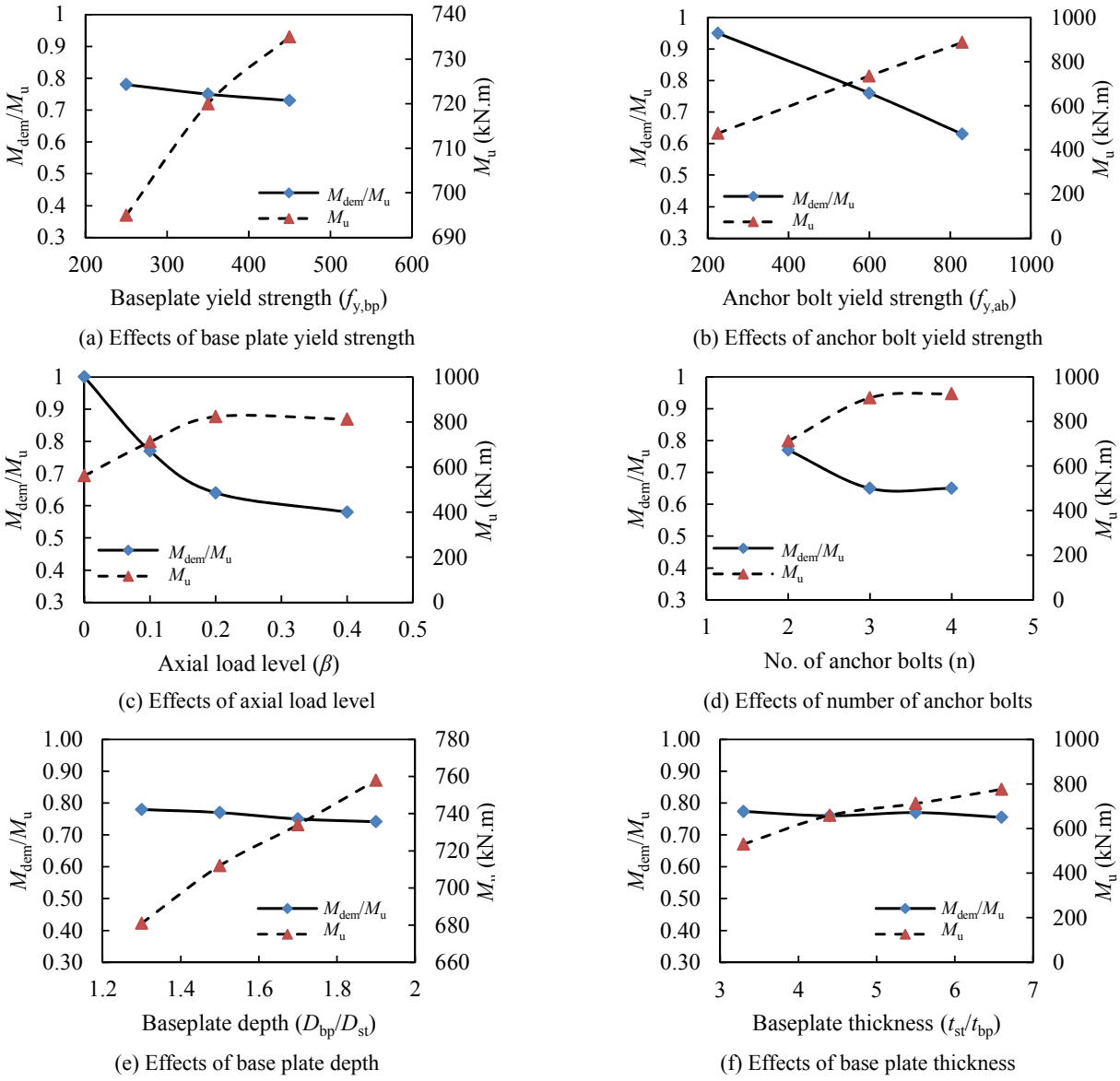


(a) Effects of base plate yield strength

(b) Effects of anchor bolt yield strength

(c) Effects of axial load level

(d) Effects of number of anchor bolts

(e) Effects of base plate depth

(f) Effects of base plate thickness

Fig. 11 Effects of various design parameters on the demountability

ratio of steel tube diameter ($D_{bp}/D_{st}$). It is observed in Fig. 9(e) that increasing base plate depth can increase the ultimate moment capacities of the connections, despite fewer influences on the initial stiffness and ductility. It should be noted that the failure modes of connections SP-14 to SP-17 are similar; with an anchor bolt yielding occurred prior to the yielding of steel tube, which is then followed by the yielding of base plate. The increase in the base plate dimension delays the yielding of base plate. However, the demountable moment capacity, which is related to the steel tube yielding, is not affected by this design parameter.

### *4.6 Effects of base plate thickness*

In order to investigate the effects of base plate thickness on the moment-rotation curves of bolted circular CFST column-base connections, four different base plate thicknesses ($t_{st}/t_{bp}$) were used. Similar to the effects of base plate depth, increasing base plate thickness can increase the ultimate moment capacity. The yielding of base plates followed the yielding of anchor bolts and steel tubes. Specifically, the ultimate moment capacity can be increased by 50% when increasing base plate from $t_{st}/t_{bp}$ = 3.3 to 6.6.

## 5. Results and discussion

### *5.1 Quantified demountability ($M_{dem}/M_u$)*

In the present paper, mechanical performance in terms of ultimate moment capacity is not the only design issue that will be covered. Demountability of the connections and the potential reusability of steel components are also investigated through this paper. Specifically, the demountability of the connections can be characterised by the elasticity of the major steel components. In this study, the major structural steel components include steel tubes and base plates. A typical elasticity distribution diagram of

Table 3 Prediction and comparison of initial stiffness and moment capacity

| Specimen | $S_{j,EC4}$[1] | $S_{j,Rigid}$[2] | $S_{j,FEM}$ | $S_{j,FEM}/S_{j,EC4}$ | $S_{j,FEM}/S_{j,Rigid}$ | $M_{EC4}$[1] | $M_{FEM}$ | $M_{FEM}/M_{EC4}$ |
|---|---|---|---|---|---|---|---|---|
| | $1\times10^6$ kN.m/rad | | | - | | kN.m | | - |
| PS-1 | 0.34 | 1.54 | 1.40 | 4.12 | 0.91 | 708 | 695 | 0.98 |
| PS-2 | 0.36 | 1.54 | 1.40 | 3.89 | 0.91 | 708 | 720 | 1.02 |
| PS-3 | 0.38 | 1.54 | 1.34 | 3.53 | 0.87 | 708 | 735 | 1.04 |
| PS-4 | 0.33 | 1.54 | 1.34 | 4.06 | 0.87 | 499 | 475 | 0.95 |
| PS-5 | 0.34 | 1.54 | 1.34 | 3.94 | 0.87 | 756 | 735 | 0.97 |
| PS-6 | 0.34 | 1.54 | 1.34 | 3.94 | 0.87 | 876 | 887 | 1.01 |
| PS-7 | 0.31 | 1.54 | 0.05 | 0.16 | 0.03 | 479 | 562 | 1.17 |
| PS-8 | 0.33 | 1.54 | 1.40 | 4.24 | 0.91 | 708 | 712 | 1.01 |
| PS-9 | 0.35 | 1.54 | 1.50 | 4.29 | 0.97 | 967 | 824 | 0.85 |
| PS-10 | 0.36 | 1.54 | 1.47 | 4.08 | 0.95 | 1480 | 813 | 0.55 |
| PS-11 | 0.34 | 1.54 | 1.40 | 4.12 | 0.91 | 708 | 712 | 1.01 |
| PS-12 | 0.34 | 1.54 | 1.46 | 4.29 | 0.95 | 933 | 906 | 0.97 |
| PS-13 | 0.35 | 1.54 | 1.52 | 4.34 | 0.99 | 1150 | 925 | 0.80 |
| PS-14 | 0.36 | 1.54 | 0.81 | 2.25 | 0.53 | 689 | 681 | 0.99 |
| PS-15 | 0.34 | 1.54 | 1.40 | 4.12 | 0.91 | 708 | 712 | 1.01 |
| PS-16 | 0.33 | 1.54 | 0.65 | 1.97 | 0.42 | 727 | 734 | 1.01 |
| PS-17 | 0.32 | 1.54 | 0.54 | 1.69 | 0.35 | 746 | 758 | 1.02 |
| PS-18 | 0.26 | 1.54 | 1.09 | 4.19 | 0.71 | 708 | 530 | 0.75 |
| PS-19 | 0.31 | 1.54 | 1.25 | 4.03 | 0.81 | 708 | 659 | 0.93 |
| PS-20 | 0.34 | 1.54 | 1.40 | 4.12 | 0.91 | 708 | 712 | 1.01 |
| PS-21 | 0.37 | 1.54 | 1.57 | 4.24 | 1.02 | 708 | 776 | 1.10 |
| Mean | | | | 3.60 | 0.79 | | | 0.96 |
| Standard deviation | | | | 1.10 | 0.25 | | | 0.13 |

[1] $S_{j,EC4}$ and $M_{EC4}$ represents the initial stiffness and moment capacity obtained from the EC3 and EC4
[2] $S_{j,Rigid}$ is the limitation of rigid column-base connections based on EC4.

steel tubes and attached base plates at their failure state is shown in Fig. 10. It can be observed from the figure that the large plastic deformation normally occurred at the bottom deformed plastically close to the compression side. It ended of the steel tubes, while the base plates usually should be noted that for connection SP18, due to the thin base plate being used, the PEEQ is predicted to be significant at both compression and tension sides. In addition, stiffeners can be welded to the bottom end of steel tubes to further enhance the strength of the connection. However, connections with such design details have to include the elasticity of the stiffeners, which is not covered in this study. It can also be seen from Figs. 10(b) and (f), increasing base plate yield strength and thickness can significantly reduce PEEQ, consequently enhancing the demountability of base plates.

To further study the demountability of the connections and encourage this concept to be widely used by structural designers, the demountability of the connection is quantified with the ratio of demountable moment to ultimate moment capacity $M_{dem}/M_u$. Fig. 11 is plotted to illustrate the effects of various design parameters on the demountability of the connections. As can be seen in the figure, increasing the strength of design parameters can increase the ultimate strength of the connections. However, effects of various design parameters on the demountability of the connections are different and can be categorised into two types. The first type includes anchor bolt yield strength, axial load level and the number of anchor bolts. It should be noted that an increase in anchor bolt yield strength or the number of anchor bolts may result in an over-strength design which is not economical. On the other hand, the small number of anchor bolts cannot satisfy the seismic design requirement. Accordingly, they are expected to remain at a reasonable level to achieve maximum potential. For these design parameters, the ultimate moment capacities can be enhanced by sacrificing the demountability ($M_{dem}/M_u$) of the connections. However, for the second type that related to the base plate, such as base plate yield strength, base plate depth and thickness, the ultimate moment capacities of the connections can be increased while keeping the demountability constant to a high-level of $M_{dem}/M_u = 0.75$.

### *5.2 Prediction of rotational stiffness and moment capacity*

As indicated in Eurocode 4 (2004), initial stiffness of composite structures could be referred to that for the steel

structures. Thus, rotational stiffness ($S_{j,EC4}$) of a series of bolted circular CFST column-base connections has been calculated with similar procedures described in Eurocode 3 (2005) and presented in Table 3. In addition to the stiffness prediction based on Eurocode 3, initial stiffness of these connections obtained from the numerical analysis ($S_{j,FEM}$) was also shown in Table 3 and compared with that from design provisions.

Based on the comparison between $S_{j,EC4}$ and $S_{j,FEM}$, it can be found that the initial stiffness of the connections can be increased by increasing axial load level, the number of anchor bolts and base plate thickness. Moreover, it can be seen from the connection PS-7, the current design provision does not include the effects of axial load into the prediction of initial stiffness properly. Furthermore, it can be observed that the current method for predicting the initial stiffness of bolted circular CFST column-base connections is significant conservative. Further research should be carried out to improve the initial stiffness predictions for bolted circular CFST column-base connections. In addition, the ratio of $S_{j,FEM}/S_{j,Rigid}$ for the investigated connections indicated that the proposed design details for the bolted circular CFST column-base connections could be classified as semi-rigid.

In terms of the prediction for ultimate moment capacity, the calculated moment capacity according to Eurocode 4 agreed reasonably well with those from finite element analysis with an average value of $M_{FEM}/M_{EC4}$ as 0.96. However, noted that the proposed prediction method with respect to moment capacity is not sensitive to the high level of axial load and the number of anchor bolts. This is mainly due to the local buckling of columns was not included into the design procedures.

## 6. Conclusions

Bolted circular CFST column-base connection is one of the current methods for circular CFST column-base construction. Despite the lower stiffness and seismic resisting performance, the bolted column-base connection has its own advantages, such as ease of construction, potential demountability and subsequent reusability of steel components. In the present study, finite element model was developed and validated against the independent experimental results. Comparison between two bolted circular CFST column-base connections in terms of their mechanical performance and demountability was carried out. Results obtained from the numerical model were analysed, and the following conclusions can be drawn:

- The general behaviour of bolted circular CFST column-base connections with different design details is similar. However, considering the demountability, base plate without pre-drilled holes for demountable circular CFST column-base connection is encouraged.
- Increasing anchor bolt yield strength, the number of anchor bolt and axial load level can enhance the mechanical performance of column-base connections. Nevertheless, the demountability of the connections will be sacrificed. Thus an increase in the strength or number of anchor bolts alone is not economical for the design of circular CFST column-base connections.
- On the contrary, increasing base plate yield strength, depth and thickness does not only increase the strength of the column-base connections but also keeps the demountability of the connections to a high level.
- Comparison in terms of initial stiffness and moment capacity with codes of practice indicates the prediction of moment capacity is reasonably accurate. To predict the initial stiffness of the bolted circular CFST column-base connections accurately, further research should be conducted.

## Acknowledgments

The research described in this paper is financially supported by the Australian Research Council (ARC) under its Discovery Scheme (Project No: DP140102134). The financial support is gratefully acknowledged.

## References

ABAQUS (2012), ABAQUS standard user's manual, Version 6.12, Dassault Systèmes Corp., Providence, RI, USA.

ACI-318 (2008), Building code requirements for reinforced concrete; Detroit, MI, USA.

Ali, A., Kim, D. and Cho, S.G. (2013), "Modelling of nonlinear cyclic load behaviour of I-shaped composite steel-concrete shear walls of nuclear power plants", *Nucl. Eng. Technol.*, **45**(1), 89-98.

Architectural Institute of Japan (AIJ) (1987), Structural calculations of steel reinforced concrete structures, Tokyo, Japan.

Aslani, F., Uy, B., Tao, Z. and Mashiri, F. (2015), "Behaviour and design of composite columns incorporating compact high-strength steel plates", *J. Constr. Steel Res.*, **107**, 94-110.

Aslani, F., Uy, B., Kang, W.H. and Hicks, S.J. (2016), "Statistical calibration of safety factors for flexural stiffness of composite columns", *Steel Compos. Struct., Int. J.*, **20**(1), 127-145.

ATC-24 (1992), "Guidelines for cyclic seismic testing of components of steel structures for buildings; Report No. ATC-24", *Applied Technology Council*, Redwood City, CA, USA.

Bruneau, M. and Marson, J. (2004), "Seismic design of concrete-filled circular steel bridge piers", *ASCE, J. Bridge Eng.*, **9**(1), 24-34.

Ellobody, E., Young, B. and Lam, D. (2006), "Behaviour of normal and high strength concrete-filled compact steel tube circular stub columns", *J. Constr. Steel Res.*, **62**, 706-715.

Eurocode 3, Part 1-8 (2005), Design of steel structures – Design of joints, European Committee for Standardisation, Brussel, Belgium.

Eurocode 4 (2004), Design of composite steel and concrete structures, part 1.1: General rules and rules for buildings. BS EN 1994-1-1: 2004: London, UK.

Gorgolewski, M. (2006), "The implications of reuse and recycling for the design of steel buildings", *Can. J. Civil Eng.*, **33**(4), 489-496.

Han, L.H. (2004), "Flexural behaviour of concrete-filled steel tubes", *J. Constr. Steel Res.*, **60**(2), 313-337.

Hitaka, T., Suita, K. and Kato, M. (2003), "CFST column base

design and practice in Japan", *Proceedings of the International Workshop on Steel and Concrete Composite Construction* (*IWSCCC-2003*); Report No. NCREE-0.-0.26, National Centre for Research in Earthquake Engineering, Taipei, Taiwan.

Hsu, H.L. and Lin, H.W. (2006), "Improving seismic performance of concrete-filled tube to base connections", *J. Constr. Steel Res.*, **62**, 1333-1340.

Jia, L.J. and Kuwamura, H. (2014), "Prediction of cyclic behaviours of mild steel at large plastic strain using coupon tests results", *ASCE J. Struct. Eng.*, **140**(2), 441-454.

Kim, H.J., Hu, J.W. and Hwang, W.S. (2015), "Cyclic testing for structural detail improvement of CFT column-foundation connections", *Sustainability*, **7**, 5260-5281.

Lehman, D.E. and Roeder, C.W. (2012), "Foundation connections for circular concrete-filled tubes", *J. Constr. Steel Res.*, **78**, 212-225.

Li, D., Uy, B. Patel, V.I. and Aslani, F. (2016a), "Behaviour and design of demountable steel column-column connections", *Steel Compos. Struct., Int. J.*, **22**(2), 428-429.

Li, D., Uy, B., Aslani, F. and Patel, V.I. (2016b), "Analysis and design of demountable steel column-baseplate connections", *Steel Compos. Struct., Int. J.*, **22**(4), 753-775.

Li, D., Uy, B., Patel, V.I. and Aslani, F. (2017a), "Analysis and design of demountable embedded steel column base connections", *Steel Compos. Struct., Int. J.*, **23**(3), 303-315.

Li, D., Uy, B., Aslani, F. and Patel, V. (2017b), "Behaviour and design of demountable CFST column-column connections under tension", *J. Constr. Steel Res.*, **138**, 761-773.

Li, D., Uy, B., Patel, V. and Aslani, F. (2018), "Behaviour and design of demountable CFST column-column connections subjected to compression", *J. Constr. Steel Res.*, **141**, 262-274.

Mirza, O. and Uy, B. (2010), "Behaviour of composite beam-column flush end-plate connections subjected to low-probability, high-consequence loading", *Eng. Struct.*, **33**(2), 647-662.

Moon, J., Roeder, C.W., Lehman, D.E. and Lee, H.E. (2012), "Analytical modeling of bending of circular concrete-filled steel tubes", *Eng. Struct.*, **42**, 349-361.

Moynihan, M.C. and Allwood, J.M. (2014), "Viability and performance of demountable composite connectors", *J. Constr. Steel Res.*, **99**, 47-56.

Rehman, N., Lam, D., Dai, X. and Ashour, A.F. (2016), "Experimental study on demountable shear connectors in composite slabs with profiled decking", *J. Constr. Steel Res.*, **122**, 178-189.

Silvestre, E., Mendiguren, J., Galdos, L. and Argandoña, E. (2015), "Comparison of the hardening behaviour of different steel families: from mild and stainless steel to advanced high strength steels", *Int. J. Mech. Sci.*, **101-102**, 10-20.

Stephens, M.T., Lehman, D.E. and Roeder, C.W. (2016), "Design of CFST column-to-foundation/cap beam connections for moderate and high seismic regions", *Eng. Struct.*, **122**, 323-337.

Tao, Z., Wang, Z.B. and Yu, Q. (2013), "Finite element modelling of concrete-filled steel stub columns under axial compression", *J. Constr. Steel Res.*, **89**, 121-131.

Thai, H.T. and Uy, B. (2015), "Finite element modelling of blind bolted composite joints", *J. Constr. Steel Res.*, **112**, 339-353.

Uy, B. (2001a), "Axial compressive strength of short steel and composite columns fabricated with high-strength steel plate", *Steel Compos. Struct., Int. J.*, **1**(2), 113-134.

Uy, B. (2001b), "Strength of short concrete filled high-strength steel box columns", *J. Constr. Steel Res.*, **57**, 113-134.

Uy, B. (2014), "Innovative connections for the demountability and rehabilitation of steel", *Space and Composite Structures*, Prague, Czech Republic.

Uy, B., Tao, Z. and Han, L.H. (2011), "Behaviour of short and slender concrete-filled stainless steel tubular columns", *J. Constr. Steel Res.*, **67**, 360-378.

Winters-Downey, E. (2010), "Reclaimed structural steel and LEED Credit MR-3 – Materials Reuse", Modern Steel Construction.

Xiao, Y., Zhang, Z.X., Hu, J.H., Kunnath, S.K. and Guo, P.X. (2011), "Seismic behaviour of CFT column and steel pile footings", *J. Bridge Eng.*, **16**(5), 575-586.

Xiong, M.X., Xiong, D.X. and Liew, J.Y.R. (2017), "Flexural performance of concrete filled tubes with high tensile steel and ultra-high strength concrete", *J. Constr. Steel Res.*, **132**,191-202.

*DL*